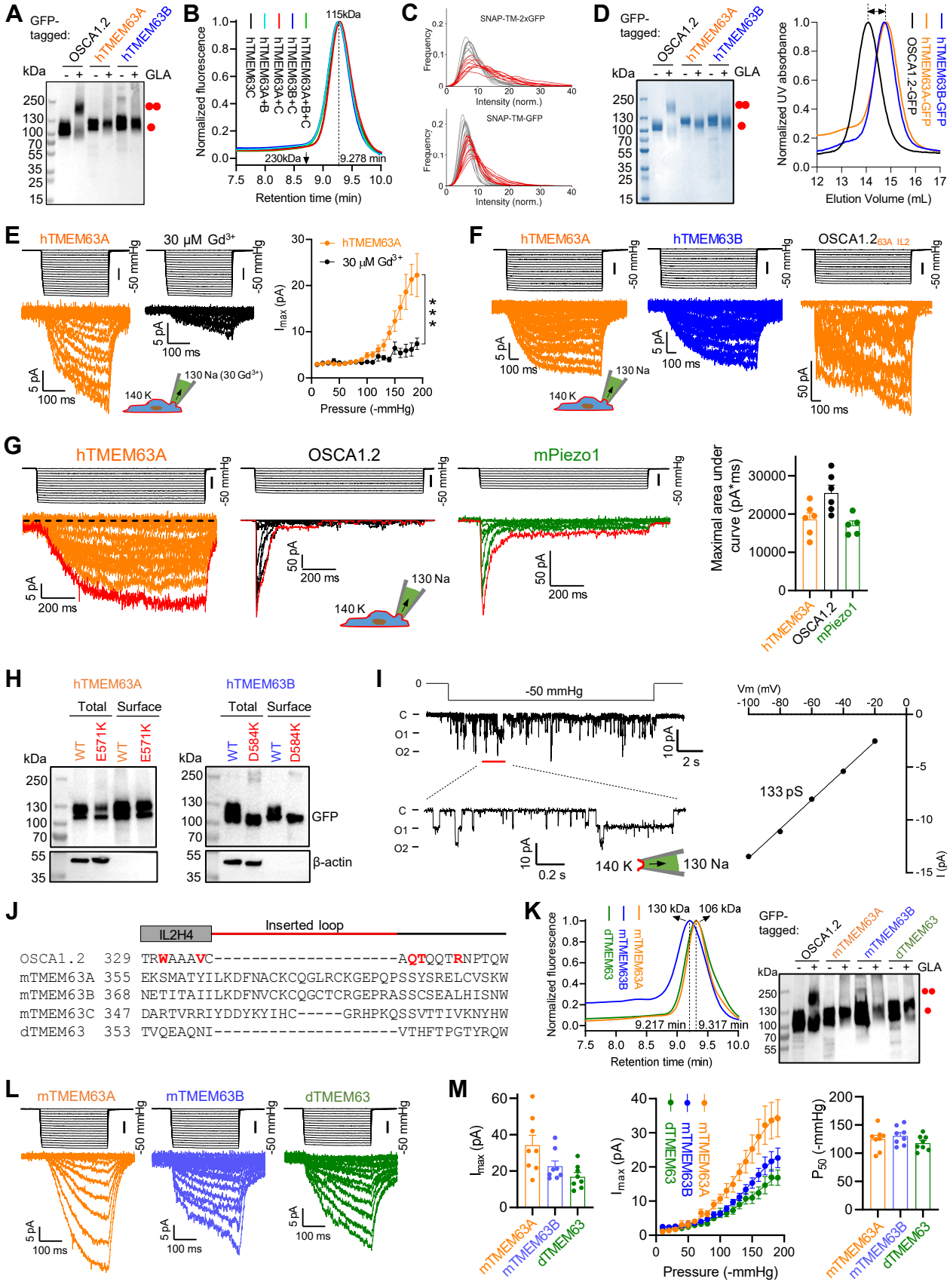
A
GFP-tagged:
OSCA1.2
hTMEM63A
hTMEM63B
kDa
GLA
250
130
100
70
55
35
25
15
B
Normalized fluorescence
hTMEM63C
hTMEM63A+B
hTMEM63A+C
hTMEM63B+C
hTMEM63A+B+C
115kDa
230kDa
9.278 min
Retention time (min)
C
SNAP-TM-2xGFP
SNAP-TM-GFP
Frequency
Intensity (norm.)
D
GFP-tagged:
OSCA1.2
hTMEM63A
hTMEM63B
kDa
GLA
Normalized UV absorbance
OSCA1.2-GFP
hTMEM63A-GFP
hTMEM63B-GFP
Elution Volume (mL)
E
hTMEM63A
30 μM Gd3+
-50 mmHg
5 pA
100 ms
140 K
130 Na (30 Gd3+)
Imax (pA)
Pressure (-mmHg)
***
F
hTMEM63A
hTMEM63B
OSCA1.263A IL2
130 Na
G
hTMEM63A
OSCA1.2
mPiezo1
50 pA
200 ms
130 Na
Maximal area under curve (pA*ms)
H
hTMEM63A
hTMEM63B
Total
Surface
WT
E571K
D584K
kDa
GFP
β-actin
I
-50 mmHg
C
O1
O2
10 pA
2 s
0.2 s
140 K
130 Na
Vm (mV)
133 pS
I (pA)
J
IL2H4
Inserted loop
OSCA1.2 329 TRWAAAVC----------AQTQQTRNPTQW
mTMEM63A 355 EKSMATYILKDFNACKCQGLRCKGEPQPSSYSRELCVSKW
mTMEM63B 368 NETITAIILKDFNVCKCQGCTCRGEPRASSCSEALHISNW
mTMEM63C 347 DARTVRRIYDDYKYIHC-----GRHPKQSSVTTIVKNYHW
dTMEM63 353 TVQEAQNI----------VTHFTPGTYRQW
K
130 kDa
106 kDa
9.217 min
9.317 min
Retention time (min)
GFP-tagged:
OSCA1.2
mTMEM63A
mTMEM63B
dTMEM63
kDa
GLA
L
mTMEM63A
mTMEM63B
dTMEM63
-50 mmHg
5 pA
100 ms
M
Imax (pA)
Pressure (-mmHg)
P50 (-mmHg)

Figure S1. Biochemical and electrophysiological analyses of TMEM63 and OSCA1.2 proteins, related to Figures 1, 4 and 5.

(A) Representative western blot of HEK293T cell lysate with overexpression of GFP-tagged OSCA1.2, hTMEM63A or hTMEM63B. The cell lysate was treated with or without 10 mM GLA.

(B) Representative FSEC traces of HEK293T cell lysate containing expression of C-terminal GFP-tagged hTMEM63C or indicated co-expression. Retention time corresponding to a potential homo- or hetero-dimer (around 230 kDa without GFP) is marked.

(C) Intensity distribution before (red) and after (gray) photobleaching for control proteins with a monomeric transmembrane (TM) domain, and either one or two GFP tags fused to their intracellular C-termini. The control proteins also contain an N-terminal SNAP tag.

(D) *Left*, coomassie-blue staining of purified OSCA1.2, human TMEM63A and TMEM63B with a C-terminal GFP-tag after SDS-PAGE. Proteins were treated with or without 10 mM GLA; *Right*, representative SEC traces of indicated purified proteins. The UV absorbance is normalized to the peak amplitude for a better comparison.

(E) *Left*, representative stretch-activated current traces from TMEM63A-expressing HEK293T cells in the absence or presence of 30 μM Gd^{3+} in the pipette solution; *Right*, quantification of I_{max} at various negative pressures in the absence (N = 7) or presence of Gd^{3+} (N = 7). $^{***}p<0.001$. Two-way ANOVA analysis.

(F) Representative stretch-activated current traces with prolonged application of negative pressures (1 s).

(G) *Left*, representative traces of stretch-activated currents in HEK293T cells with overexpression of hTMEM63A, OSCA1.2 or mouse Piezo1; *Right*, quantification of the maximal area under the current traces, which represents the number of conducted charges.

(H) Biotinylation assay detecting both the total expression and cell surface expression of hTMEM63A WT and E571K mutant (*Left*) or hTMEM63B WT and D584K mutant (*Right*) in HEK293T cells.

(I) *Left*, representative trace of single-channel recordings of OSCA1.2 reconstituted in liposomes. The voltage was held at -50 mV. Closed (C) and open (O) states are indicated; *Right*, current-voltage relationship of stretch-activated single-channel currents. The calculated single-channel conductance is shown.

(J) Sequence alignment of the region within IL2 that mediates dimerization of OSCA1.2. Residues that directly mediate OSCA1.2 dimerization are highlighted in red. The inserted loop in TMEM63s is indicated by the red line.

(K) Representative FSEC traces (*Left*) or western blot (*Right*) of HEK293T cell lysate with overexpression of GFP-tagged mouse TMEM63A (mTMEM63A), TMEM63B (mTMEM63B) or *Drosophila melanogaster* TMEM63 (dTMEM63). Cell lysates were treated without (-) or with (+) 10 mM GLA.

(L) Representative traces of stretch-activated currents (-80 mV) from HEK293T cells with overexpression of mTMEM63A, mTMEM63B or dTMEM63.

(M) Quantification of I_{max} (*Left*) and P_{50} (*Right*) from each individual patches; *Middle*, averaged pressure-response current curves fitted with a Boltzmann equation (mTMEM63A, N = 8; mTMEM63B, N = 8; dTMEM63, N = 8).

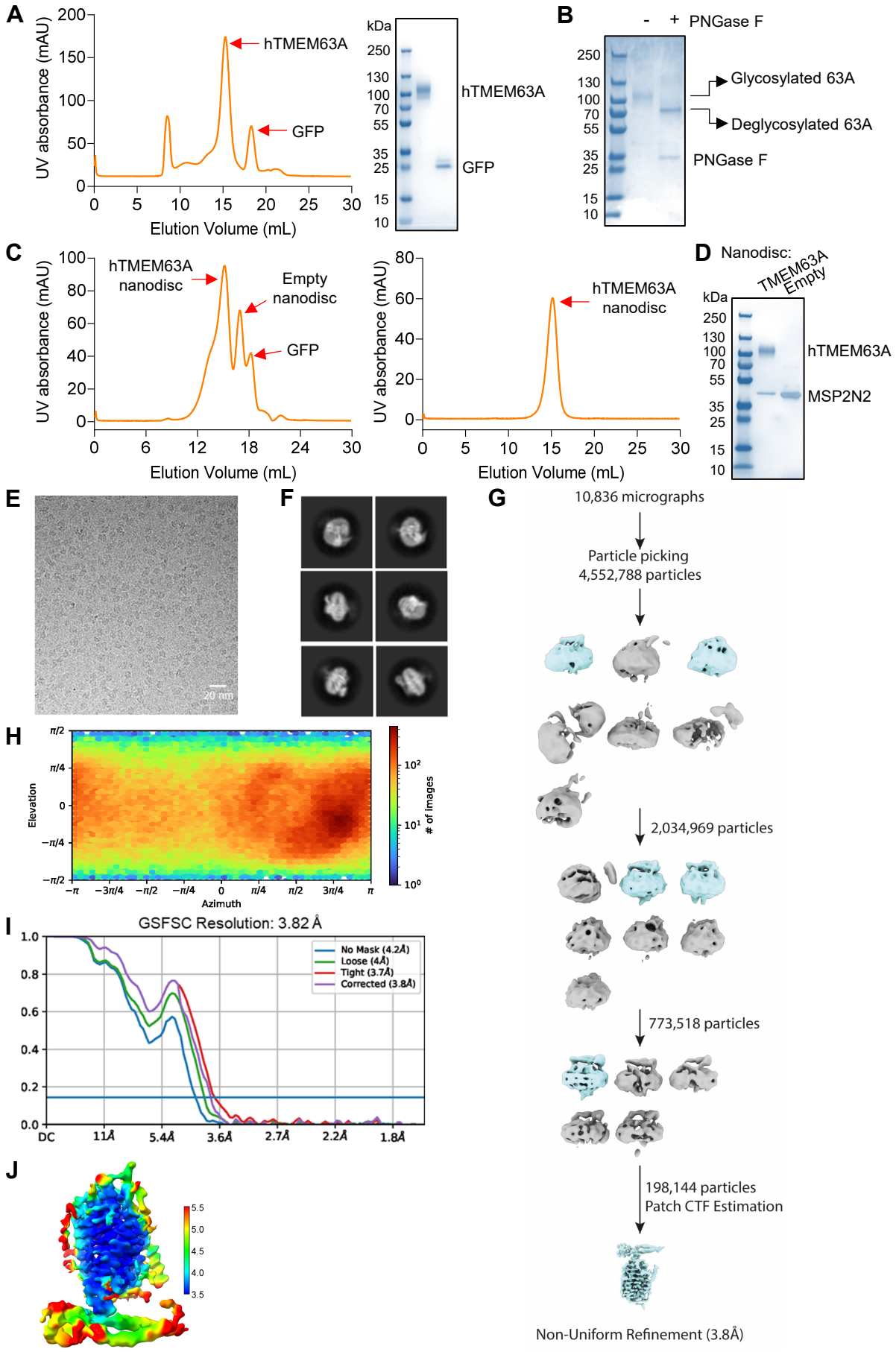
A
UV absorbance (mAU)
Elution Volume (mL)
hTMEM63A
GFP
kDa
hTMEM63A
GFP
B
- + PNGase F
Glycosylated 63A
Deglycosylated 63A
PNGase F
C
hTMEM63A nanodisc
Empty nanodisc
GFP
hTMEM63A nanodisc
D
Nanodisc:
TMEM63A
Empty
hTMEM63A
MSP2N2
E
20 nm
F
G
10,836 micrographs
Particle picking
4,552,788 particles
2,034,969 particles
773,518 particles
198,144 particles
Patch CTF Estimation
Non-Uniform Refinement (3.8Å)
H
Elevation
Azimuth
# of images
I
GSFSC Resolution: 3.82 Å
No Mask (4.2Å)
Loose (4Å)
Tight (3.7Å)
Corrected (3.8Å)
J

Figure S2. Purification and reconstruction of human TMEM63A, related to Figure 2.

(A) *Left*, representative SEC trace of purified human TMEM63A protein in LMNG/CHS, treated with 3C protease to cleave GFP. The peak fractions corresponding to hTMEM63A and GFP are indicated; *Right*, SDS-PAGE gel staining of hTMEM63A and GFP peak fractions.

(B) SDS-PAGE gel staining of hTMEM63A peak fraction treated without or with PNGase F. Glycosylated and deglycosylated hTMEM63A are indicated.

(C) *Left*, SEC trace of hTMEM63A reconstituted in lipid nanodiscs with MSP2N2; *Right*, SEC trace of hTMEM63A nanodisc peak fraction collected from the *left* panel.

(D) SDS-PAGE gel staining of peak fractions of hTMEM63A nanodiscs and empty nanodiscs.

(E and F) Representative cryo-EM raw image (E) and 2D-class averages (F) of hTMEM63A in nanodiscs.

(G) Cryo-EM data processing flowchart for nanodisc-embedded hTMEM63A density map.

(H) Angular distribution of reconstructed particles in the final map of hTMEM63A.

(I) FSC plots of unmasked and masked maps.

(J) Final reconstruction map colored by local resolution.

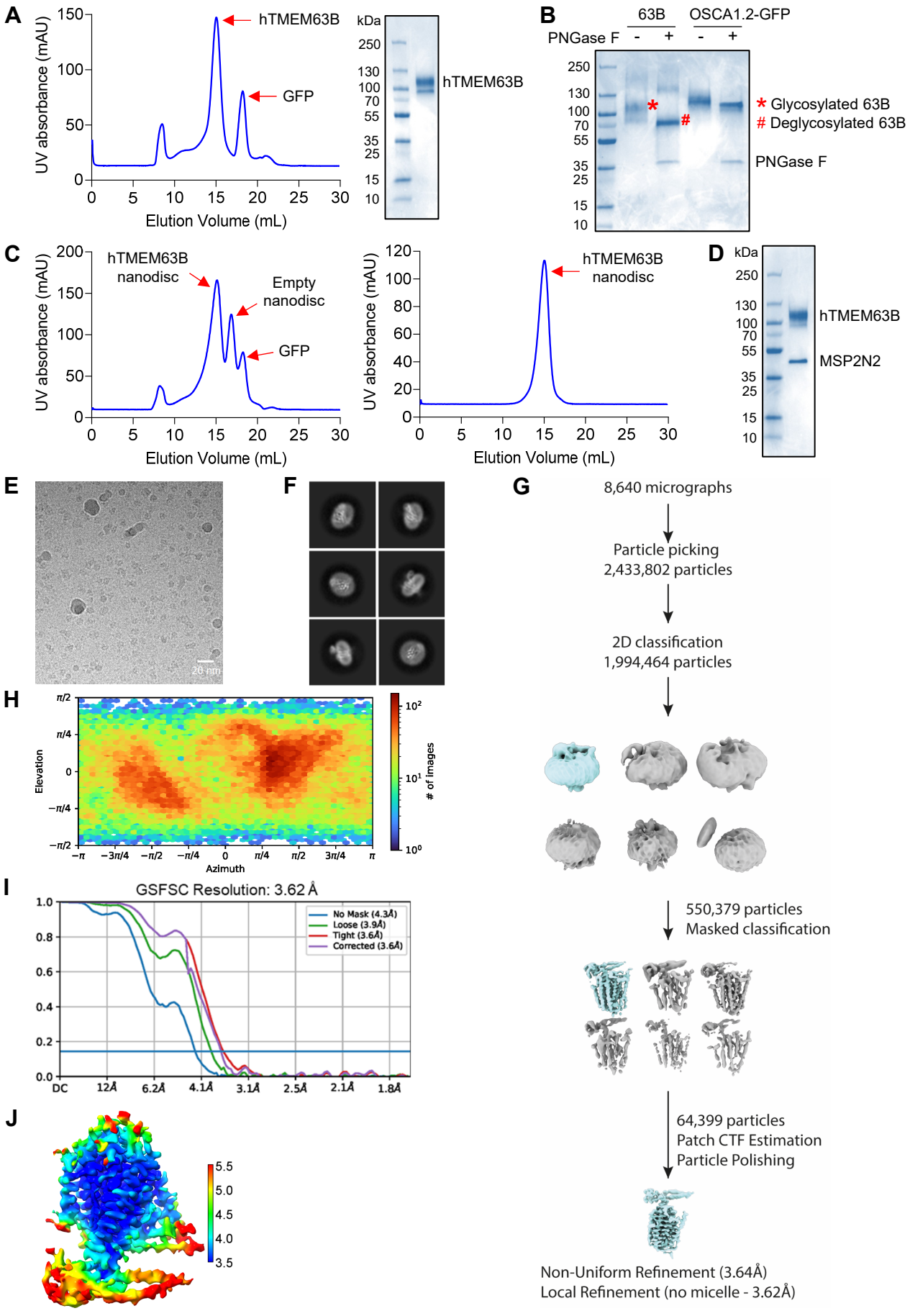
A
UV absorbance (mAU)
Elution Volume (mL)
hTMEM63B
GFP
kDa
hTMEM63B
B
63B
OSCA1.2-GFP
PNGase F
* Glycosylated 63B
# Deglycosylated 63B
PNGase F
C
hTMEM63B nanodisc
Empty nanodisc
GFP
hTMEM63B nanodisc
D
hTMEM63B
MSP2N2
E
20 nm
F
G
8,640 micrographs
Particle picking
2,433,802 particles
2D classification
1,994,464 particles
550,379 particles
Masked classification
64,399 particles
Patch CTF Estimation
Particle Polishing
Non-Uniform Refinement (3.64Å)
Local Refinement (no micelle - 3.62Å)
H
Elevation
Azimuth
# of images
I
GSFSC Resolution: 3.62 Å
No Mask (4.3Å)
Loose (3.9Å)
Tight (3.6Å)
Corrected (3.6Å)
J

Figure S3. Purification and reconstruction of human TMEM63B, related to Figure 2.

(A) SEC trace of purified human TMEM63B protein in LMNG/CHS. GFP was cleaved by 3C protease treatment. The hTMEM63B peak fraction was examined by SDS-PAGE.

(B) SDS-PAGE gel staining of purified hTMEM63B and OSCA1.2-GFP treated without or with PNGase F. Glycosylated and deglycosylated hTMEM63B are indicated.

(C) *Left*, SEC trace of hTMEM63B reconstituted in lipid nanodiscs with MSP2N2; *Right*, SEC trace of hTMEM63B nanodisc peak fraction collected from the *left* panel.

(D) SDS-PAGE gel staining of the hTMEM63B nanodisc peak fraction.

(E and F) Representative cryo-EM raw image (E) and 2D-class averages (F) of hTMEM63B in LMNG/CHS.

(G) Cryo-EM data processing flowchart for the map of hTMEM63B in LMNG/CHS.

(H) Angular distribution of reconstructed particles in the final map of hTMEM63B.

(I) FSC plots of unmasked and masked maps.

(J) Final reconstruction map colored by local resolution.

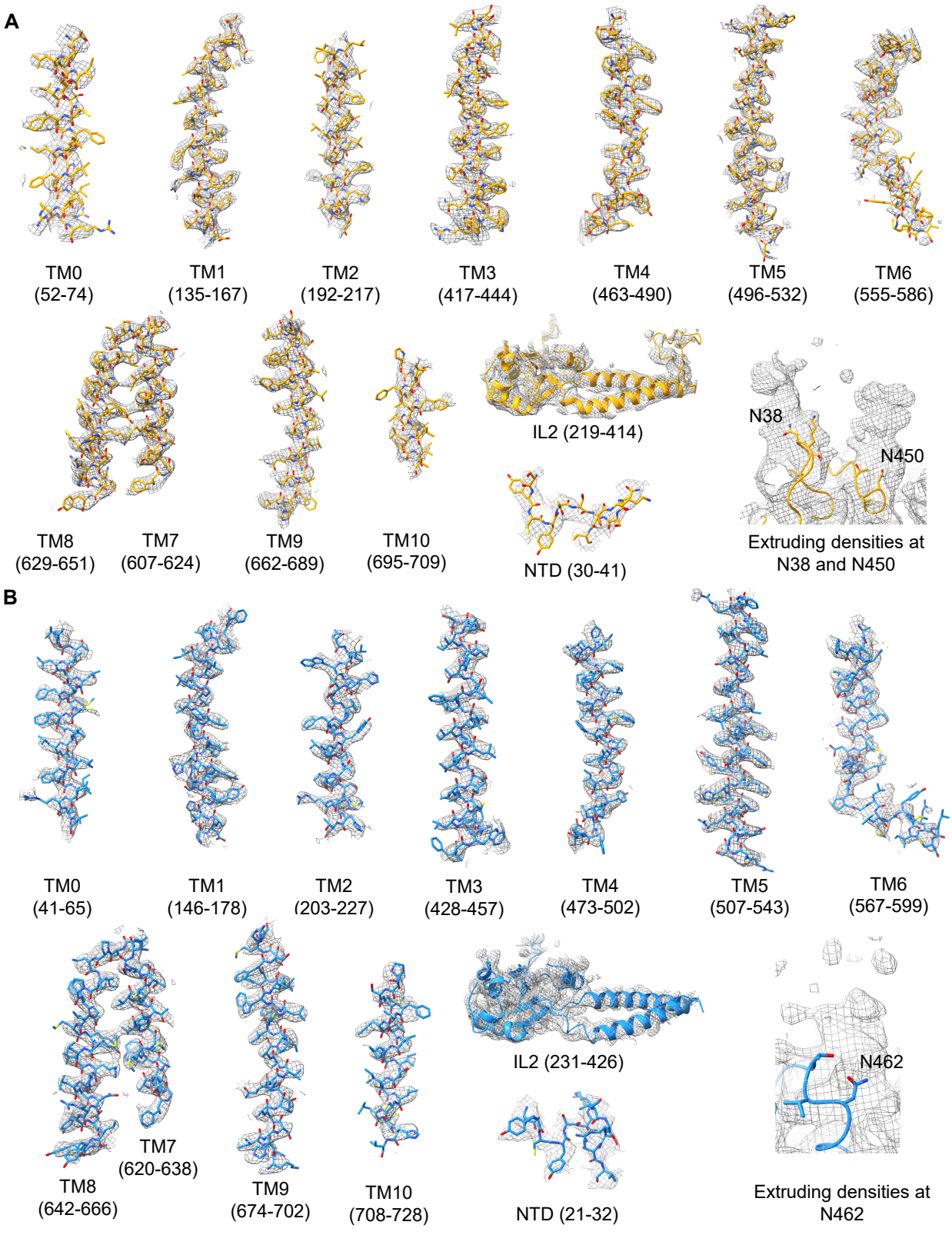

Figure S4. Cryo-EM density and fit with models of TMEM63s, related to Figure 2.
(A and B) Selected regions of cryo-EM map of TMEM63A in nanodiscs (A) and TMEM63B in LMNG (B) superimposed with the atomic models.

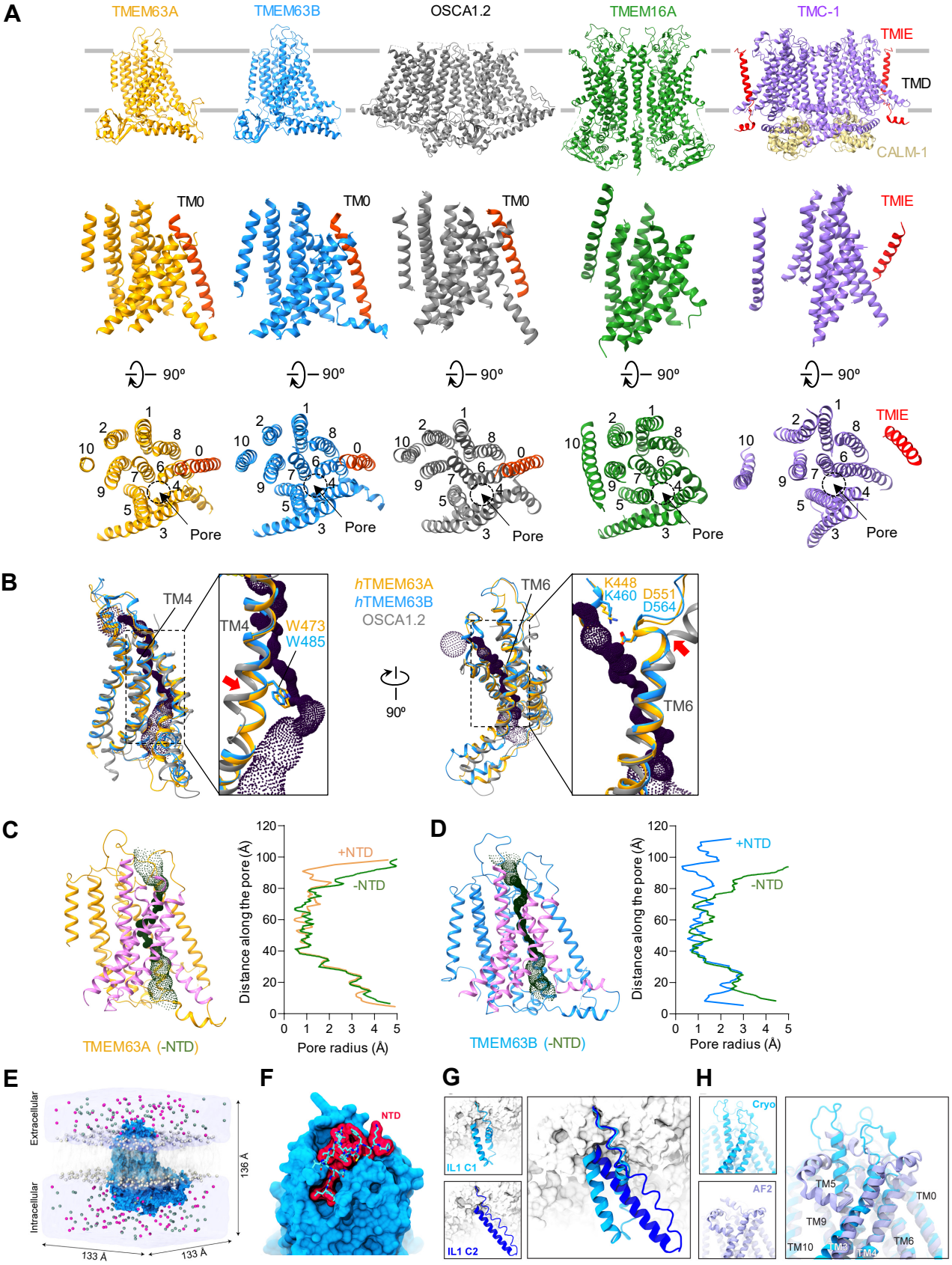
A
TMEM63A
TMEM63B
OSCA1.2
TMEM16A
TMC-1
TMIE
TMD
CALM-1
TM0
90°
Pore
B
TM4
W473
W485
hTMEM63A
hTMEM63B
OSCA1.2
TM6
K448
K460
D551
D564
C
TMEM63A (-NTD)
+NTD
-NTD
Distance along the pore (Å)
Pore radius (Å)
D
TMEM63B (-NTD)
E
Extracellular
Intracellular
136 Å
133 Å
F
NTD
G
IL1 C1
IL1 C2
H
Cryo
AF2
TM5
TM0
TM9
TM10
TM3
TM4
TM6

Figure S5. Structural comparisons and ion permeation pore analysis, related to Figures 3.

(A) Comparison of TMDs. *Upper*, side view of ribbon structures of human TMEM63A, human TMEM63B, *Arabidopsis thaliana* OSCA1.2 (PDB: 6MGV), mouse TMEM16A (PDB: 5OYG) and *C. elegans* TMC1 bound with TMIE and CALM-1 (PDB: 7USX). *Middle*, side-view of ribbon structures of TMD isolated from TMEM63A, TMEM63B, OSCA1.2, TMEM16A and TMC-1. The TM0 in TMEM63A, TMEM63B and OSCA1.2 and TMIE is highlighted in red. *Lower*, top view of the TMD with the location of putative ion permeation pore indicated.

(B) Structural comparisons of the pore domain among TMEM63A, TMEM63B and OSCA1.2 (PDB: 6MGV). The noticeable differences in TM4 and TM6 were highlighted.

(C and D) Effects of NTD on the ion permeation pore profile in TMEM63A and TMEM63B. *Left*, ribbon structures of TMEM63A (C) and TMEM63B (D) without the NTD (S30-V45 in TMEM63A; P19-L36 in TMEM63B). The calculated pore profile is shown as green dots. Pore lining TMs are colored in magenta; *Right*, pore radii of TMEM63A (C) and TMEM63B (D) with (+NTD) and without NTD (-NTD) against distance along the pore.

(E) All-atom MD simulation setup for TMEM63B in a POPC membrane (Sim1a). Protein is shown in surface representation. Chloride and potassium ions are in dark green and pink, respectively. Lipid phosphates are white spheres and water is in transparent blue surface.

(F) Highlight of TMEM63B NTD, removed in some simulations.

(G) Two predicted conformations for IL1.

(H) Experimentally derived (Cryo) and AlphaFold2 predicted (AF2) conformations of extracellular regions of TM3-TM4 and TM5-TM6. Other helices (e.g., TM0, TM9, TM10) have matching conformations.

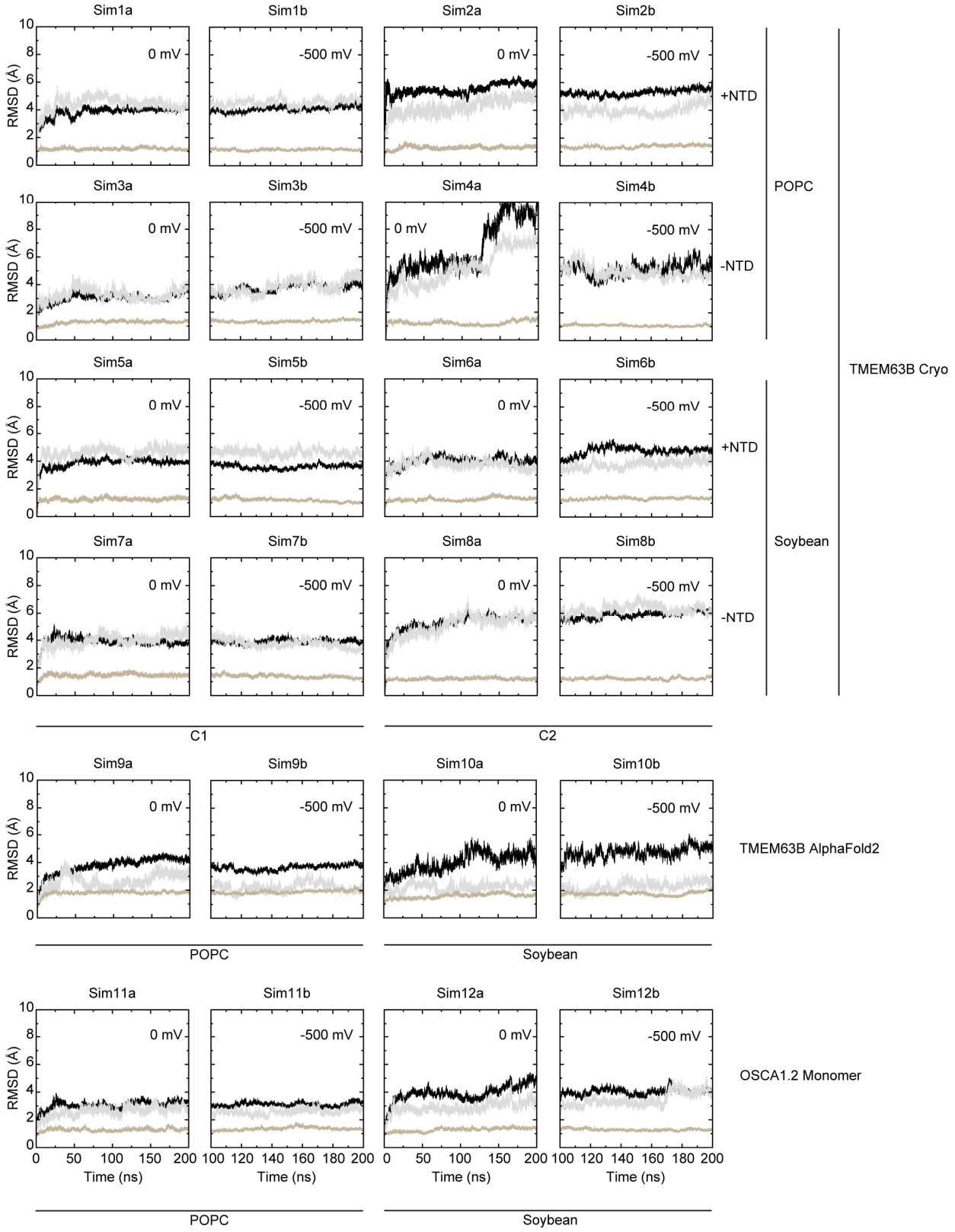

Figure S6. Domain stability in simulations, related Figure 3.

RMSD values for all simulations in Table S2 computed using Cα atoms of the entire protein (black), of the IL2 (gray), and of the TMD (tan).

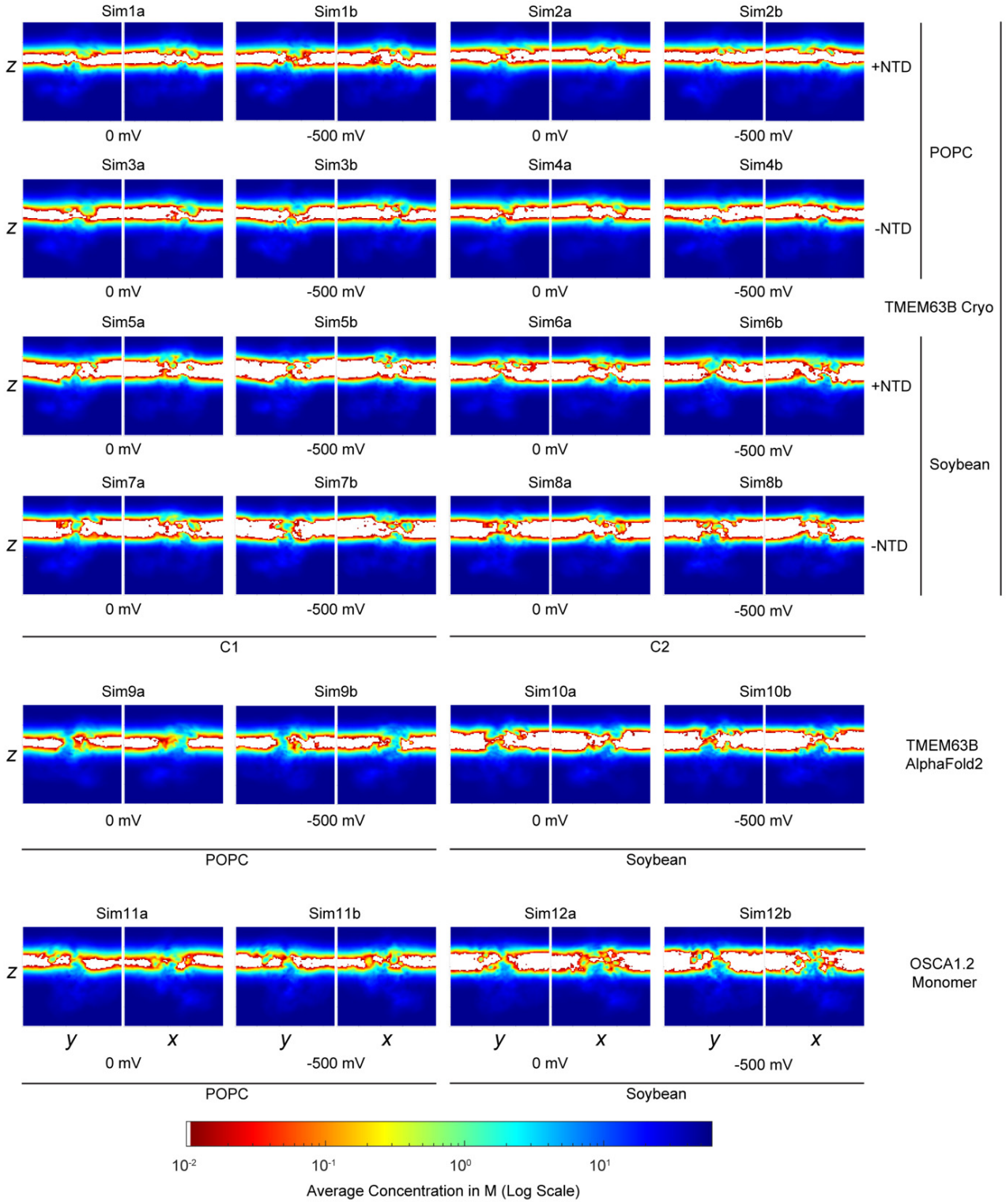

Figure S7. Pore hydration in simulations of TMEM63B and OSCA1.2, related to Figure 3. Two dimensional slices showing time- and space-averaged water concentrations for all MD simulations listed in Table S2. Data shown in a logarithmic color scale to highlight transient hydration of putative pores.

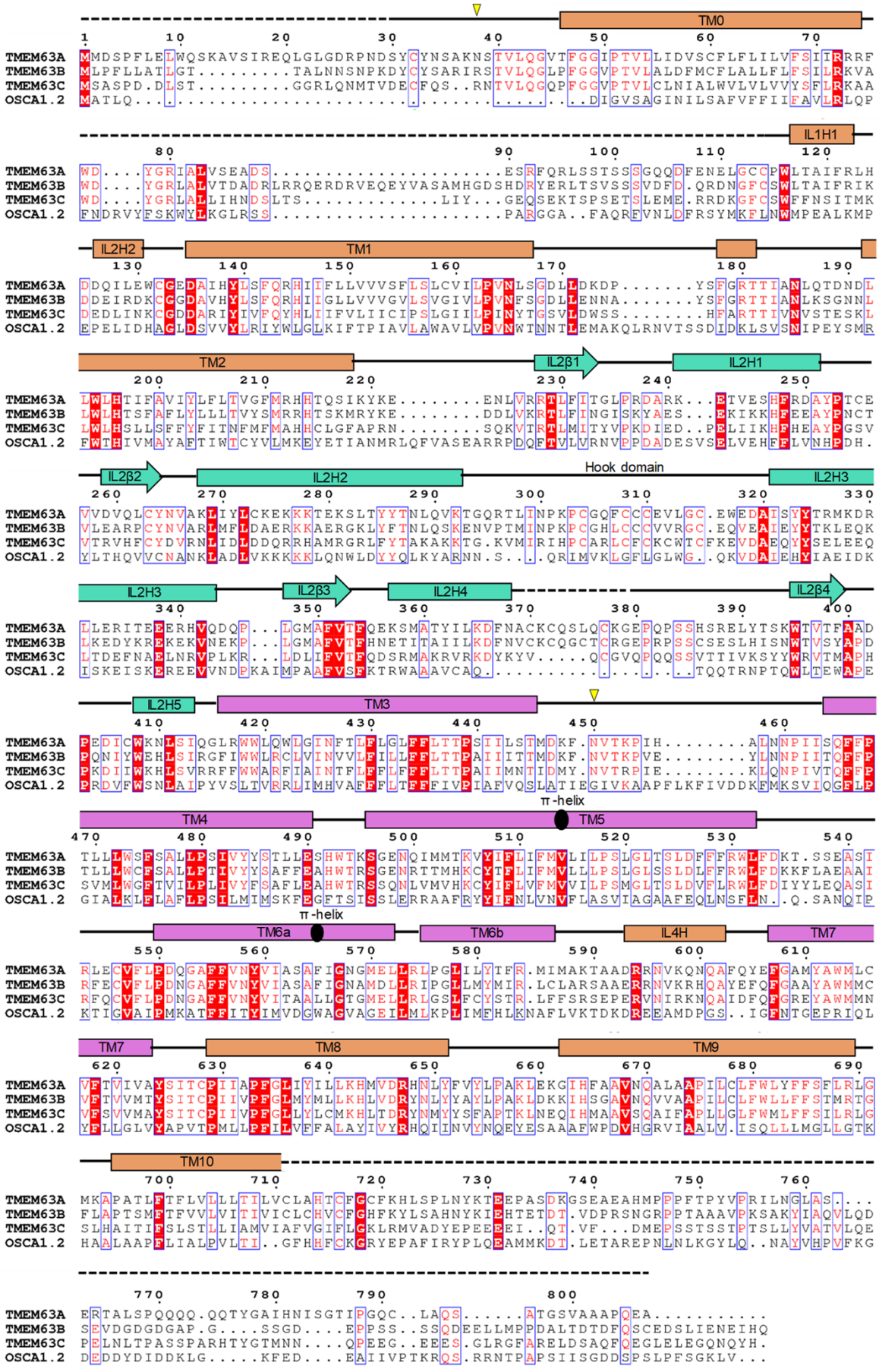
TM0
IL1H1
IL2H2
TM1
TM2
IL2β1
IL2H1
IL2β2
IL2H2
Hook domain
IL2H3
IL2H3
IL2β3
IL2H4
IL2β4
IL2H5
TM3
π-helix
TM4
TM5
π-helix
TM6a
TM6b
IL4H
TM7
TM7
TM8
TM9
TM10
TMEM63A
TMEM63B
TMEM63C
OSCA1.2

Figure S8. Protein sequence alignment of TMEM63 proteins and OSCA1.2, related to Figures 2 and 7.

Multiple sequence alignment was performed using ClustalW for human TMEM63A (UniProt Accession #: O94886), TMEM63B (Q5T3F8), TMEM63C (Q9P1W3) and *Arabidopsis thaliana* OSCA1.2 (Q5XEZ5). Secondary elements of human TMEM63A based on cryo-EM model is shown on the top, with the same color code as in Figure 2C. Unresolved regions in the cryo-EM model are indicated with dashed line. Two putative *N*-linked glycosylation sites (N38 and N450) in hTMEM63A are indicated with yellow triangles. The π-helix in TM5 and TM6 is labeled with a black oval.

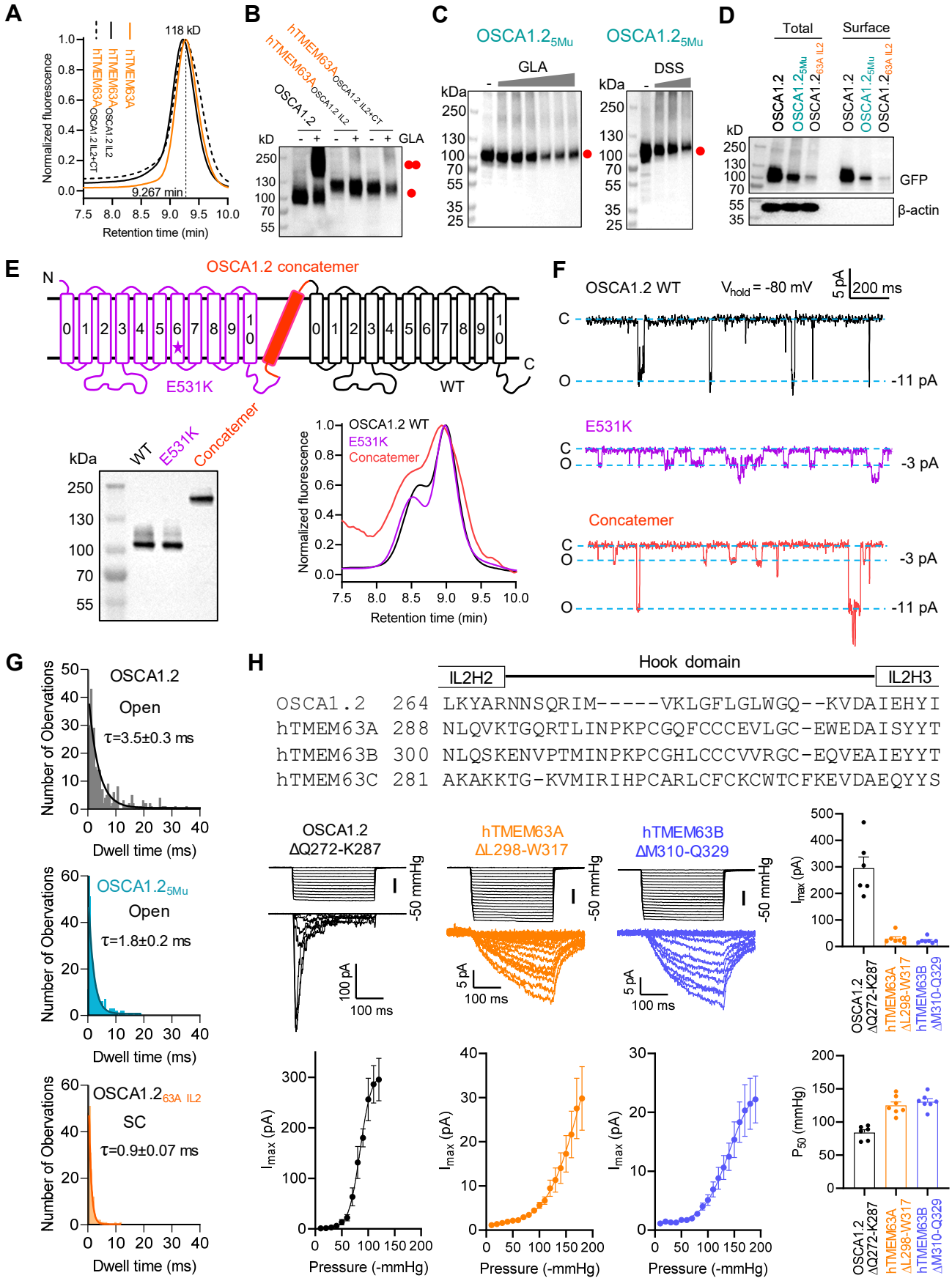
A
118 kD
hTMEM63A
hTMEM63A-OSCA1.2 IL2
hTMEM63A-OSCA1.2 IL2-CT
Normalized fluorescence
9.267 min
Retention time (min)
B
hTMEM63A-OSCA1.2 IL2-CT
hTMEM63A-OSCA1.2 IL2
OSCA1.2
kD
GLA
C
OSCA1.2 5Mu
GLA
DSS
kDa
D
Total
Surface
OSCA1.2
OSCA1.2 5Mu
OSCA1.2 63A IL2
GFP
β-actin
E
OSCA1.2 concatemer
N
C
E531K
WT
kDa
WT
E531K
Concatemer
OSCA1.2 WT
E531K
Concatemer
Normalized fluorescence
Retention time (min)
F
OSCA1.2 WT
V hold = -80 mV
5 pA
200 ms
C
O
-11 pA
E531K
-3 pA
Concatemer
-3 pA
-11 pA
G
OSCA1.2
Open
τ=3.5±0.3 ms
Number of Obervations
Dwell time (ms)
OSCA1.2 5Mu
Open
τ=1.8±0.2 ms
OSCA1.2 63A IL2
SC
τ=0.9±0.07 ms
H
IL2H2
Hook domain
IL2H3
OSCA1.2 264 LKYARNNSQRIM-----VKLGFLGLWGQ--KVDAIEHYI
hTMEM63A 288 NLQVKTGQRTLINPKPCGQFCCCEVLGC-EWEDAISYYT
hTMEM63B 300 NLQSKENVPTMINPKPCGHLCCCVVRGC-EQVEAIEYYT
hTMEM63C 281 AKAKKTG-KVMIRIHPCARLCFCKCWTCFKEVDAEQYYS
OSCA1.2 ΔQ272-K287
hTMEM63A ΔL298-W317
hTMEM63B ΔM310-Q329
-50 mmHg
100 pA
100 ms
5 pA
I max (pA)
Pressure (-mmHg)
P 50 (mmHg)

Figure S9. Characterization of engineered OSCA1.2, TMEM63A and TMEM63B channels, related to Figures 5 and 6.

(A and B) Representative FSEC traces (A) and western blot (B) of HEK293T cell lysate with overexpression of GFP-tagged constructs, as indicated. hTMEM63A$_{OSCA1.2\ IL2}$, IL2 of hTMEM63A were replaced with OSCA1.2 IL2; hTMEM63A$_{OSCA1.2\ IL2+CT}$, both IL2 and C-terminus of hTMEM63A were replaced with those of OSCA1.2. Cell lysates were treated without (-) or with (+) 10 mM GLA.

(C) Representative western blots of GFP-tagged OSCA1.2$_{5Mu}$ overexpressed in HEK293T cells. *Left*, cell lysates were treated with GLA as in Figure 5F; *Right*, intact cells were treated with DSS as in Figure 1D.

(D) Biotinylation assay detecting both the total expression and cell surface expression in HEK293T cells overexpressing GFP-tagged OSCA1.2, OSCA1.2$_{5Mu}$ and OSCA1.2$_{63A\ IL2}$.

(E) *Upper*, diagram showing the design of OSCA1.2 concatemer. E531K mutant (purple, the mutation site is indicated with a star) and WT (black) protomers are connected via a single transmembrane helix of glycophorin A (red); *Lower*, representative western blot (*Left*) and FSEC traces (*Right*) of HEK293T cell lysates with overexpression of GFP-tagged OSCA1.2 WT, E531K mutant or the concatemer.

(F) Representative traces of stretch-activated single-channel currents recorded at -80 mV. The closed (C) and open (O) states, and amplitude of unitary currents are indicated.

(G) Dwell time histograms for the fully open state of OSCA1.2 and OSCA1.2$_{5Mu}$, and the assumed sub-conductance state of OSCA1.2$_{63A\ IL2}$.

(H) *Upper*, sequence alignment of the hook domain; *Middle*, representative traces of stretch-activated currents (-80 mV) from HEK293T cells with overexpression of Hook-deleted OSCA1.2 (ΔQ272-K287), hTMEM63A (ΔL298-W317) or hTMEM63B (ΔM310-Q329), and quantification of I_{max}; *Lower*, averaged pressure-response current curves fitted with a Boltzmann equation (OSCA1.2 ΔQ272-K287, N = 6; hTMEM63A ΔL298-W317, N = 7; hTMEM63B ΔM310-Q329, N = 7) and quantification of P_{50} from each individual patches.

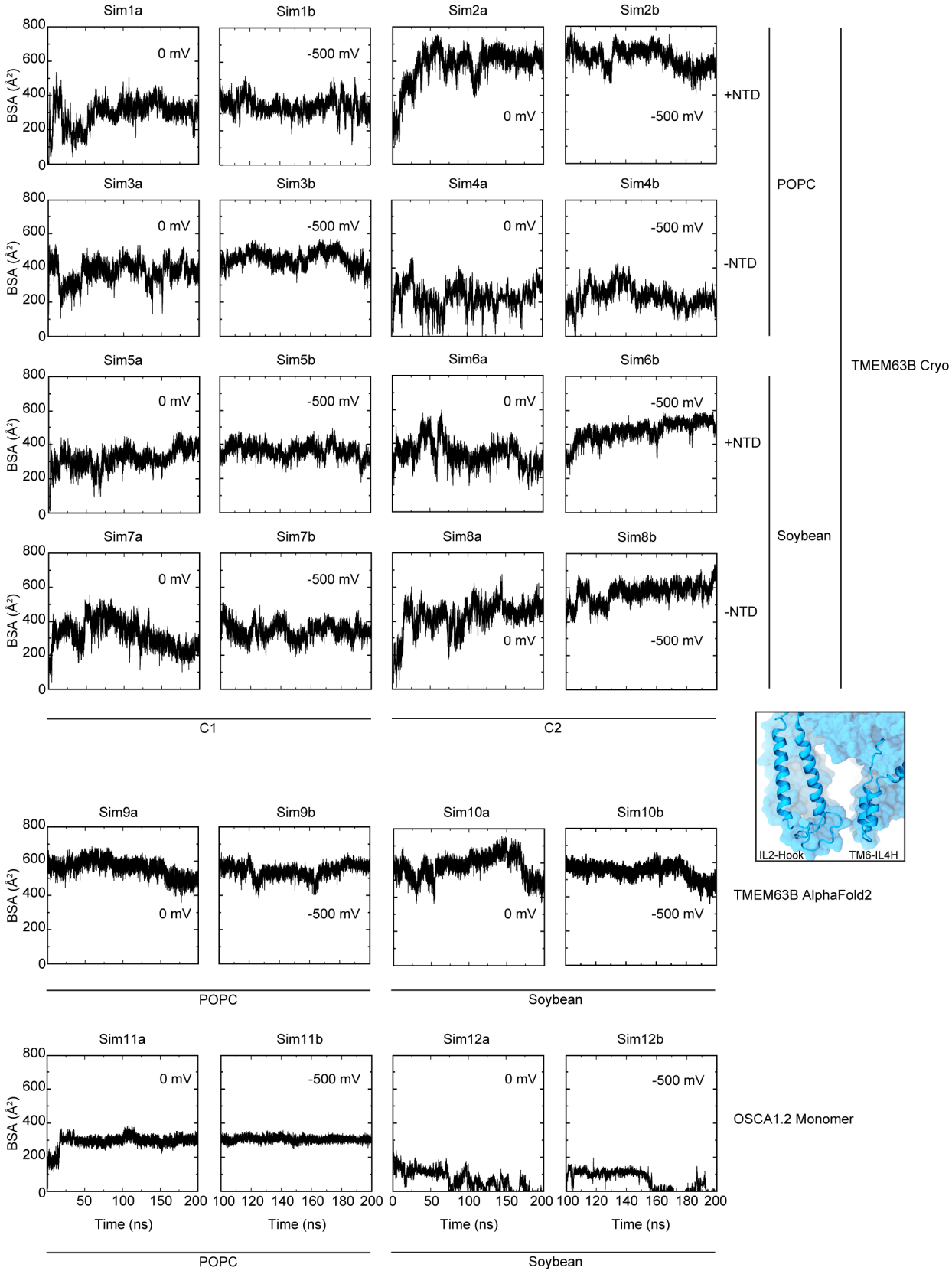
Sim1a
Sim1b
Sim2a
Sim2b
Sim3a
Sim3b
Sim4a
Sim4b
Sim5a
Sim5b
Sim6a
Sim6b
Sim7a
Sim7b
Sim8a
Sim8b
Sim9a
Sim9b
Sim10a
Sim10b
Sim11a
Sim11b
Sim12a
Sim12b
0 mV
-500 mV
BSA (Å²)
0
200
400
600
800
+NTD
-NTD
POPC
Soybean
TMEM63B Cryo
C1
C2
IL2-Hook
TM6-IL4H
TMEM63B AlphaFold2
OSCA1.2 Monomer
50
100
150
200
100
120
140
160
180
200
Time (ns)

Figure S10. Predicted contacts between the IL2 domain and helices TM6b and ILH4, related to Figure 6.

Buried surface area (BSA) is used to quantify the interaction between the IL2 hook and the TM6b and IL4H region near the bottom of the pore for TMEM63B and OSCA1.2 models. Inset image shows top view of this interaction in the TMEM63B cryo-EM model used for simulations (middle right). Initial BSA values were ~20 $Å^2$ for the TMEM63B cryo-EM model, ~600 $Å^2$ for the TMEM63B AlphaFold2 model, and ~260 $Å^3$ for OSCA1.2. Values shown for all simulations listed in Table S2.

Table S1. Cryo-EM data collection, refinement and validation statistics , related to STAR Methods.

	TMEM63A in nanodiscs (EMD-28153) (PDB 8EHW)	TMEM63A in LMNG	TMEM63B in nanodiscs	TMEM63B in LMNG (EMD-28154) (PDB 8EHX)
Data collection/processing				
Magnification	105,000	36,000	105,000	105,000
Voltage (kV)	300	200	300	300
Electron exposure ($e^-/Å^2$)	50.705	52.563	53.048	53.048
Defocus range (μm)	-1 to -2	-1.4 to -2.5	-0.8 to -2.1	-0.8 to -2.1
Number of frames	50	50	50	50
Pixel size (Å)	0.825	1.1	0.825	0.825
Micrographs (no.)	10,836			8,640
Initial particles (no.)	4,552,788			2,433,802
Final particles (no.)	198,144			64,399
Symmetry imposed	C1			C1
Map resolution (Å)	3.82			3.62
FSC threshold	0.143			0.143
Map sharpening B factor ($Å^2$)	-198.6			-131.2
Refinement				
Initial model	AlphaFold 2			AlphaFold 2
Model resolution (Å)	4.03			3.87
FSC threshold	0.5			0.5
Model composition				
Non-hydrogen atoms	5150			5153
Protein residues	630			631
R.m.s. deviations				
Bond lengths (Å)	0.003			0.003
Bond angles (°)	0.769			0.648
Validation				
MolProbity score	2.19			2.13
Clashscore	15.33			13.01
Poor rotamers (%)	0.18%			0
Ramachandran plot				
Favored (%)	91.67%			91.33%
Allowed (%)	8.33%			8.51%
Disallowed (%)	0			0.16%

Table S2. Simulations summary for each system, related to STAR Methods.

C1 and C2 indicate the conformation of IL1 predicted by AF2 multimer prediction and monomer prediction, respectively.

Label	Protein	Membrane	NTD	IL1	Voltage (mV)	Length (ns)	Start	# atoms	Dimensions (Å^3)
Sim1a	TMEM63B (Cryo)	POPC	+	C1	0	200	-	205,840	133 × 133 × 136
Sim1b					-500	100	Sim1a (100 ns)		
Sim2a				C2	0	200	-	211,763	135 × 135 × 142
Sim2b					-500	100	Sim2a (100 ns)		
Sim3a			-	C1	0	200	-	209,874	135 × 135 × 138
Sim3b					-500	100	Sim3a (100 ns)		
Sim4a				C2	0	200	-	209,954	133 × 133 × 136
Sim4b					-500	100	Sim4a (100 ns)		
Sim5a		Soybean	+	C1	0	200	-	203,823	133 × 133 × 136
Sim5b					-500	100	Sim5a (100 ns)		
Sim6a				C2	0	200	-	205,514	135 × 135 × 142
Sim6b					-500	100	Sim6a (100 ns)		
Sim7a			-	C1	0	200	-	203,993	135 × 135 × 142
Sim7b					-500	100	Sim7a (100 ns)		
Sim8a				C2	0	200	-	204,024	133 × 133 × 136
Sim8b					-500	100	Sim8a (100 ns)		
Sim9a	TMEM63B (AlphaFold2)	POPC	+	C2	0	200	-	200,163	135 × 135 × 135
Sim9b					-500	100	Sim9a (100 ns)		
Sim10a		Soybean			0	200	-	209,874	135 × 135 × 135
Sim10b					-500	100	Sim10a (100 ns)		
Sim11a	OSCA1.2 Monomer (PDB: 6MGV)	POPC		-	0	200	-	187,941	130 × 133 × 132
Sim11b					-500	100	Sim11a (100 ns)		
Sim12a		Soybean			0	200	-	194,793	135 × 135 × 132
Sim12b					-500	100	Sim12a (100 ns)		
Total Simulation Time						3,600			